Channel Estimation for mmWave Satellite Communications with Reconfigurable Intelligent Surface

Jinming Zhang and Chenhao Qi
School of Information Science and Engineering
Southeast University, Nanjing, China
Email: {jmzhang, qch}@seu.edu.cn

GLOBECOM 2021 - 2021 IEEE Global Communications Conference | 978-1-7281-8104-2/21/$31.00 ©2021 IEEE | DOI: 10.1109/GLOBECOM46510.2021.9685288

***Abstract*—We consider an mmWave satellite communication system with a reconfigurable intelligent surface (RIS) to enhance the signal coverage, where both the satellite and the served users are equipped with phased arrays. Different from the existing methods that separately estimate the uplink channel from the user to the RIS and that from the RIS to the satellite, we directly estimate the cascaded channel by proposing two schemes. In the first scheme with two stages, we power off the last antennas of the satellite, user and the RIS in the first stage and then transceive some pilot symbols, while in the second stage we power off the first antennas of the satellite, user and the RIS and then transceive the same pilot symbols. Then we perform the channel estimation based on the estimating-signal-parameter-via-rotational-invariance-techniques (ESPRIT) method. In the second scheme that does not power off any antenna and needs only one stage, we propose a null space projection (NSP) algorithm, where the equivalent channel matrix is estimated through projecting the dictionary steering vectors to the null space of the received signal covariance matrices. Simulation results show that the NSP scheme needs much fewer pilots and much lower hardware complexity than the ESPRIT scheme but with some sacrifice in channel estimation performance.**

***Index Terms*—Channel estimation, millimeter wave (mmWave) communications, reconfigurable intelligent surface (RIS), satellite communications.**

I. Introduction

Satellite communications have become increasingly attractive since they can provide low-latency and reliable communication service. Compared with terrestrial wireless communications, satellite communications can provide stable signal coverage for remote areas such as plateaus, mountains and seas [1]. Moreover, the signal to noise ratio (SNR), ranging, accuracy, and anti-multipath ability can be further improved by satellite communications for those areas with terrestrial wireless communications [2]. In particular, satellite communications in the millimeter wave (mmWave) frequency band not only have the advantages as aforementioned, but also have potential to achieve high spectral efficiency by making full use of the abundant frequency resources [3]. On the other hand, the recently emerged reconfigurable intelligent surface (RIS) is capable of smartly controlling the wireless propagative environment, which can improve the signal coverage of mmWave communications by reflecting the highly directional mmWave signal to the obscured places. Compared with mmWave multiple-input multiple-output (MIMO) communications, the RIS-aided mmWave MIMO communications can achieve higher spectral efficiency [4]. But different from mmWave satellite MIMO communications using terrestrial relays [5], in the RIS-aided mmWave satellite MIMO communications, the RIS can only passively reflect incident signals instead of positively transmitting signals.

For mmWave terrestrial MIMO communications with RIS, the channel model has been well established [6] [7]. For example, a channel estimation framework with two estimation algorithms is proposed by comprehensively considering the pilots and RIS phase shifts [8]. However, to the best knowledge of the authors, the channel modeling as well as the channel estimation has not yet been investigated for mmWave satellite MIMO communications with RIS, which inspires some of our thoughts as follows.

In this work, we investigate the channel estimation for the mmWave geostationary earth orbit (GEO) satellite MIMO communication system with RIS. We apply the estimating-signal-parameter-via-rotational-invariance-techniques (ESPRIT) method to estimate the angle of arrival (AoA) and the angle of departure (AoD) in two stages. In the first stage, we power off the last antennas of the satellite, user and the RIS and transceive some pilot symbols, while in the second stage we power off the first antennas of the satellite, the user and the RIS and transceive the same pilot symbols. Then we perform the channel estimation based on the ESPRIT method. In the second scheme that needs only one stage, we propose a null space projection (NSP) algorithm, where the equivalent channel matrix is estimated through projecting the dictionary steering vectors to the null space of the received signal covariance matrices.

We use the following notations in our paper. Symbols for vectors (lower case) and matrices (upper case) are in boldface. $(\cdot)^T$, $(\cdot)^H$, $(\cdot)^{-1}$ and $(\cdot)^\dagger$ denote the transpose, conjugate transpose (Hermitian), inverse and pseudo-inverse, respectively. The set of $p \times q$ complex-valued matrices is denoted by $\mathbb{C}^{p\times q}$. $\|\cdot\|_F$ and $\mathbb{E}\{\cdot\}$ is used to denote the Frobenius norm and the expectation. $\boldsymbol{A}\otimes\boldsymbol{B}$ and $\boldsymbol{A}\odot\boldsymbol{B}$ represent the Kronecker product and the Khatri-Rao product of the matrix $\boldsymbol{A}$ and $\boldsymbol{B}$. Complex Gaussian distribution is denoted by $\mathcal{CN}$. We use $\mathrm{diag}\{\boldsymbol{a}\}$to denote the square diagonal matrix with the elements of vector

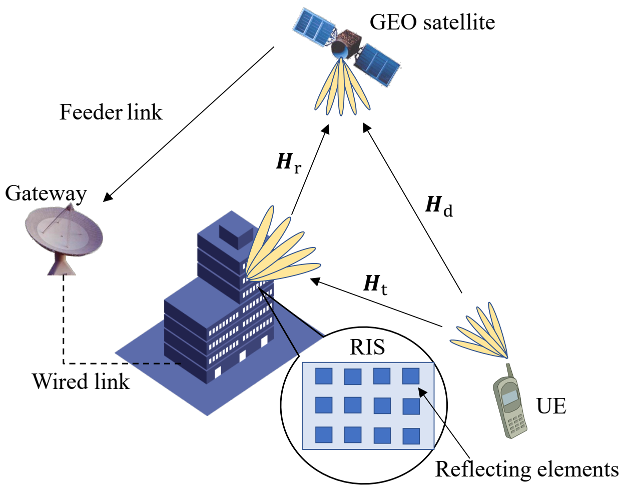

Fig. 1. MIMO mmWave GEO satellite communication system with RIS.

$\boldsymbol{a}$ on the main diagonal.

II. System Model

As shown in Fig. 1, an mmWave GEO satellite communication system includes a GEO satellite, an RIS, a user equipment (UE) and a gateway. There is a feeder link between the satellite and the gateway, enabling the gateway to transmit control signals to the satellite. The RIS is connected to the gateway via a wired link, so that the gateway can change the parameters of the RIS in real time. The RIS is equipped with many reflecting elements, which can passively reflect the incident signal. Each element of the RIS, which functions as a phase shifter on the incident signal, is independently controlled by the gateway.

We consider the uplink transmission, where the UE transmits the signal to the satellite. Assume a uniform linear array (ULA) with half wavelength interval is used by both the satellite and the UE. Denote the antenna numbers of the ULAs at the satellite and UE by N_{r} and N_{t}, respectively. Denote the number of elements of the RIS by N_{s}. Then the uplink channel between the UE and the RIS can be denoted by $\boldsymbol{H}_{\mathrm{t}} \in \mathbb{C}^{N_{\mathrm{s}} \times N_{\mathrm{t}}}$. According to the Saleh-Valenzuela channel model [9], $\boldsymbol{H}_{\mathrm{t}}$ can be expressed as

$$\boldsymbol{H}_{\mathrm{t}} = \sqrt{\frac{N_{\mathrm{s}} N_{\mathrm{t}}}{L}} \sum_{l=1}^{L} g_l \boldsymbol{\alpha}(N_{\mathrm{s}}, \theta_{\mathrm{t},l}) \boldsymbol{\alpha}^T (N_{\mathrm{t}}, \phi_{\mathrm{t},l}), \tag{1}$$

where L denotes the number of paths and g_l denotes the channel gain of the lth path obeying $g_l \sim \mathcal{CN}(0,1)$, for $l = 1, 2, \ldots, L$. $\theta_{\mathrm{t},l}$ and $\phi_{\mathrm{t},l}$ denote the AoA of the RIS and the AoD of the UE for the lth path, respectively. The channel steering vector $\boldsymbol{\alpha}(N, \theta)$ as a function of N and θ is defined as

$$\boldsymbol{\alpha}(N,\theta) \triangleq \frac{1}{\sqrt{N}} [1, e^{j\pi \cos(\theta)}, e^{j\pi 2 \cos(\theta)}, \cdots, e^{j\pi (N-1)\cos(\theta)}]^T, \tag{2}$$

where N represents the number of antennas and θ represents the AoD or the AoA.

In order to simplify the notation, we define

$$\begin{aligned} \boldsymbol{A}_{\mathrm{t}} &\triangleq \big[\boldsymbol{\alpha}(N_{\mathrm{t}}, \phi_{\mathrm{t},1}), \boldsymbol{\alpha}(N_{\mathrm{t}}, \phi_{\mathrm{t},2}), \cdots, \boldsymbol{\alpha}(N_{\mathrm{t}}, \phi_{\mathrm{t},L})\big], \\ \boldsymbol{B}_{\mathrm{t}} &\triangleq \big[\boldsymbol{\alpha}(N_{\mathrm{s}}, \theta_{\mathrm{t},1}), \boldsymbol{\alpha}(N_{\mathrm{s}}, \theta_{\mathrm{t},2}), \cdots, \boldsymbol{\alpha}(N_{\mathrm{s}}, \theta_{\mathrm{t},L})\big], \\ \boldsymbol{G}_{\mathrm{t}} &\triangleq \sqrt{\tfrac{N_{\mathrm{s}} N_{\mathrm{t}}}{L}} \mathrm{diag}\big\{[g_1, g_2, \cdots, g_L]^T\big\}. \end{aligned} \tag{3}$$

Then $\boldsymbol{H}_{\mathrm{t}}$ can be expressed as

$$\boldsymbol{H}_{\mathrm{t}} = \boldsymbol{B}_{\mathrm{t}} \boldsymbol{G}_{\mathrm{t}} \boldsymbol{A}_{\mathrm{t}}^T. \tag{4}$$

The uplink channel between the RIS and the satellite is denoted by $\boldsymbol{H}_{\mathrm{r}} \in \mathbb{C}^{N_{\mathrm{r}} \times N_{\mathrm{s}}}$. We only consider the line-of-sight (LoS) path between the RIS and the satellite while ignoring the non-line-of-sight (NLoS) paths because the difference of their gain is more than 20dB [10]. Note that the path loss in the free space can be expressed as

$$P_{\mathrm{r}} = \frac{\lambda^2 G_{\mathrm{r}} G_{\mathrm{s}}}{(4\pi)^2 d^2 \kappa T B_{\mathrm{W}}}, \tag{5}$$

where λ, G_{r}, G_{s}, d, κ, T and B_{W} represent the wavelength, the gain of each RIS element, the gain of each satellite antenna, the distance between the satellite and the RIS, the Boltzman constant, the sky noise temperature and the bandwidth, respectively [11]. Then $\boldsymbol{H}_{\mathrm{r}}$ can be written as

$$\boldsymbol{H}_{\mathrm{r}} = \sqrt{N_{\mathrm{s}} N_{\mathrm{r}} P_{\mathrm{r}}} \boldsymbol{\alpha}(N_{\mathrm{r}}, \theta_{\mathrm{r}}) \boldsymbol{\alpha}^T (N_{\mathrm{s}}, \phi_{\mathrm{s}}), \tag{6}$$

where θ_{r} represents the AoA of the satellite and ϕ_{s} represents the AoD of the RIS. Similarly, we define

$$\boldsymbol{a}_{\mathrm{r}} \triangleq \boldsymbol{\alpha}(N_{\mathrm{r}}, \theta_{\mathrm{r}}), \ \boldsymbol{b}_{\mathrm{r}} \triangleq \boldsymbol{\alpha}(N_{\mathrm{s}}, \phi_{\mathrm{s}}), \ g_{\mathrm{r}} \triangleq \sqrt{N_{\mathrm{s}} N_{\mathrm{r}} P_{\mathrm{r}}}. \tag{7}$$

Then $\boldsymbol{H}_{\mathrm{r}}$ can be rewritten as

$$\boldsymbol{H}_{\mathrm{r}} = g_{\mathrm{r}} \boldsymbol{a}_{\mathrm{r}} \boldsymbol{b}_{\mathrm{r}}^T. \tag{8}$$

The uplink channel between the UE and the satellite is denoted by $\boldsymbol{H}_{\mathrm{d}} \in \mathbb{C}^{N_{\mathrm{r}} \times N_{\mathrm{t}}}$. However, to ease the estimation of $\boldsymbol{H}_{\mathrm{d}}$, we can shortly power off the RIS. Then the estimation of $\boldsymbol{H}_{\mathrm{d}}$ is essentially a standard mmWave MIMO channel estimation problem that can be tackled by existing methods [12]. Once $\boldsymbol{H}_{\mathrm{d}}$ is estimated, we power on the RIS. When estimating the cascaded channel of $\boldsymbol{H}_{\mathrm{t}}$ and $\boldsymbol{H}_{\mathrm{r}}$, the received signal component from $\boldsymbol{H}_{\mathrm{d}}$ can be treated as a known constant, which implies the impact of $\boldsymbol{H}_{\mathrm{d}}$ can be completely removed. Therefore, in this work, we focus on the estimation of the cascaded channel.

Suppose $\boldsymbol{H}_{\mathrm{r}}$ and $\boldsymbol{H}_{\mathrm{t}}$ keep constant within K consecutive time slots, under the block fading assumption for wireless channels. Further suppose the transceiving of each pilot vector occupies a time slot. We transmit P different pilot vectors, where each pilot vector is repetitively transmitted in S consecutive time slots. We model the RIS as a diagonal matrix $\mathrm{diag}\{\boldsymbol{q}_s\}$, where $\boldsymbol{q}_s \triangleq [e^{-j\beta_1}, e^{-j\beta_2}, \cdots, e^{-j\beta_{N_{\mathrm{s}}}}]^T \in \mathbb{C}^{N_{\mathrm{s}}}$ is a phase shifting vector in the sth time slot for $s = 1, 2, \ldots, S$. We set $K = PS$. Then the received signal by the satellite with the pth pilot vector and the sth phase shifting vector for $p = 1, 2, \ldots, P$ and $s = 1, 2, \ldots, S$ can be expressed as

$$\boldsymbol{Y}_{p,s} = \boldsymbol{W}^T \boldsymbol{H}_{\mathrm{r}} \mathrm{diag}\{\boldsymbol{q}_s\} \boldsymbol{H}_{\mathrm{t}} \boldsymbol{f}_p + \boldsymbol{W}^T \boldsymbol{M}_{p,s}, \tag{9}$$

$$\boldsymbol{R}_1 = \begin{bmatrix} \boldsymbol{a}_\mathrm{r} & \boldsymbol{a}_\mathrm{r} & \cdots & \boldsymbol{a}_\mathrm{r} \\ e^{j\pi\phi_{\mathrm{t},1}}\boldsymbol{a}_\mathrm{r} & e^{j\pi\phi_{\mathrm{t},2}}\boldsymbol{a}_\mathrm{r} & \cdots & e^{j\pi\phi_{\mathrm{t},L}}\boldsymbol{a}_\mathrm{r} \\ \vdots & \vdots & \ddots & \vdots \\ e^{j(N_t-2)\pi\phi_{\mathrm{t},1}}\boldsymbol{a}_\mathrm{r} & e^{j(N_t-2)\pi\phi_{\mathrm{t},2}}\boldsymbol{a}_\mathrm{r} & \cdots & e^{j(N_t-2)\pi\phi_{\mathrm{t},L}}\boldsymbol{a}_\mathrm{r} \end{bmatrix} \tag{15}$$

$$\boldsymbol{R}_2 = \begin{bmatrix} e^{j\pi\phi_{\mathrm{t},1}}\boldsymbol{a}_\mathrm{r} & e^{j\pi\phi_{\mathrm{t},2}}\boldsymbol{a}_\mathrm{r} & \cdots & e^{j\pi\phi_{\mathrm{t},L}}\boldsymbol{a}_\mathrm{r} \\ e^{j2\pi\phi_{\mathrm{t},1}}\boldsymbol{a}_\mathrm{r} & e^{j2\pi\phi_{\mathrm{t},2}}\boldsymbol{a}_\mathrm{r} & \cdots & e^{j2\pi\phi_{\mathrm{t},L}}\boldsymbol{a}_\mathrm{r} \\ \vdots & \vdots & \ddots & \vdots \\ e^{j(N_t-1)\pi\phi_{\mathrm{t},1}}\boldsymbol{a}_\mathrm{r} & e^{j(N_t-2)\pi\phi_{\mathrm{t},2}}\boldsymbol{a}_\mathrm{r} & \cdots & e^{j(N_t-1)\pi\phi_{\mathrm{t},L}}\boldsymbol{a}_\mathrm{r} \end{bmatrix} \tag{17}$$

---

where $\boldsymbol{W} \in \mathbb{C}^{N_\mathrm{r}\times N_\mathrm{RF}}$, N_RF, $\boldsymbol{f}_p \in \mathbb{C}^{N_\mathrm{t}}$ and $\boldsymbol{M}_{p,s} \in \mathbb{C}^{N_\mathrm{r}}$ denote the combine matrix at the satellite, the number of radio frequency (RF) chains at the satellite, the transmitting signals at the UE and the additive white Gaussian noise vector, respectively [8].

If we stack the signals of PS time slots in a matrix $\boldsymbol{Y} \in \mathbb{C}^{(N_\mathrm{RF}P)\times S}$, it can be written as

$$\boldsymbol{Y} = \begin{bmatrix} \boldsymbol{Y}_{1,1} & \boldsymbol{Y}_{1,2} & \cdots & \boldsymbol{Y}_{1,S} \\ \boldsymbol{Y}_{2,1} & \boldsymbol{Y}_{2,2} & \cdots & \boldsymbol{Y}_{2,S} \\ \vdots & \vdots & \ddots & \vdots \\ \boldsymbol{Y}_{P,1} & \boldsymbol{Y}_{P,2} & \cdots & \boldsymbol{Y}_{P,S} \end{bmatrix}. \tag{10}$$

Then we have

$$\boldsymbol{Y} = (\boldsymbol{F}^T \otimes \boldsymbol{W}^T)\boldsymbol{H}\boldsymbol{Q} + \boldsymbol{M}, \tag{11}$$

where $\boldsymbol{F} = [\boldsymbol{f}_1, \boldsymbol{f}_2, \cdots, \boldsymbol{f}_P]$ and $\boldsymbol{Q} = [\boldsymbol{q}_1, \boldsymbol{q}_2, \cdots, \boldsymbol{q}_S]$. $\boldsymbol{M}$ is the additive white Gaussian noise stacked by $\boldsymbol{W}^T\boldsymbol{M}_{p,s}$ similarly. $\boldsymbol{H}$ is the equivalent channel matrix, which can be written as

$$\boldsymbol{H} = \boldsymbol{H}_\mathrm{t}^T \odot \boldsymbol{H}_\mathrm{r} = g_\mathrm{r}(\boldsymbol{A}_\mathrm{t} \otimes \boldsymbol{a}_\mathrm{r})\boldsymbol{G}_\mathrm{t}(\boldsymbol{B}_\mathrm{t}^T \odot \boldsymbol{b}_\mathrm{r}^T). \tag{12}$$

III. Channel Estimation for the mmWave GEO Satellite system with RIS

According to (9)(11), the cascaded channel estimation problem is to estimate $\boldsymbol{H}_\mathrm{t}$ and $\boldsymbol{H}_\mathrm{r}$ independently or estimate the equivalent channel matrix $\boldsymbol{H}$. The direct solution is to use the least square (LS) solution

$$\widehat{\boldsymbol{H}}_\mathrm{LS} = (\boldsymbol{F}^T \otimes \boldsymbol{W}^T)^\dagger \boldsymbol{Y}\boldsymbol{Q}^\dagger. \tag{13}$$

However, it requires that the number of the time slots should satisfies $PS \geq \frac{N_\mathrm{r}N_\mathrm{s}N_\mathrm{t}}{N_\mathrm{RF}}$. Such solution is almost impractical in the system because the large number of time slots means the long channel coherence time and processing delay which can not be well addressed. In the next two subsections, we proposes a ESPRIT based channel estimation algorithm in the mmWave MIMO GEO satellite communication system with RIS and a channel estimation algorithm using the projection on the null space which needs fewer pilots and lower hardware complexity.

A. Two-stage ESPRIT based channel estimation

ESPRIT is widely used in array signal processing, especially in the AoD and AoA estimation [12]. In this subsection, we apply ESPRIT for the mmWave MIMO GEO satellite communication system with RIS to estimate the AoA and AoD of the RIS, the AoD of the UE and the AoA of the satellite. This method requires two stages, which means the number of time slots is $2PS$. In fact, the estimation of the AoA and AoD at the RIS, UE and the satellite has the same mathematical formulation. Thus, we take the AoD at the UE as an example.

For the first stage, we power off the last antenna at the UE and the received signal can be expressed as

$$\begin{aligned} \boldsymbol{X}_1 &= g_\mathrm{r}(\boldsymbol{F}_1^T \otimes \boldsymbol{W}^T)(\boldsymbol{A}_\mathrm{t} \otimes \boldsymbol{a}_\mathrm{r})\boldsymbol{G}_\mathrm{t}(\boldsymbol{B}_\mathrm{t}^T \odot \boldsymbol{b}_\mathrm{r}^T)\boldsymbol{Q} \\ &= g_\mathrm{r}(\widetilde{\boldsymbol{F}}^T \otimes \boldsymbol{W}^T)\boldsymbol{R}_1\boldsymbol{G}_\mathrm{t}(\boldsymbol{B}_\mathrm{t}^T \odot \boldsymbol{b}_\mathrm{r}^T)\boldsymbol{Q}, \end{aligned} \tag{14}$$

where $\widetilde{\boldsymbol{F}} \in \mathbb{C}^{P\times(N_\mathrm{t}-1)}$. $\boldsymbol{F}_1$ is the transmitting pilots matrix satisfying $\boldsymbol{F}_1 = [\widetilde{\boldsymbol{F}}, \boldsymbol{0}]^T$. The matrix $\boldsymbol{R}_1$ can be written as (15). For simplicity, we ignore the noise term $\boldsymbol{M}$ here.

Similarly, for the second stage, we power off the first antenna at the UE and the received signal can be expressed as

$$\begin{aligned} \boldsymbol{X}_2 &= g_\mathrm{r}(\boldsymbol{F}_2^T \otimes \boldsymbol{W}^T)(\boldsymbol{A}_\mathrm{t} \otimes \boldsymbol{a}_\mathrm{r})\boldsymbol{G}_\mathrm{t}(\boldsymbol{B}_\mathrm{t}^T \odot \boldsymbol{b}_\mathrm{r}^T)\boldsymbol{Q} \\ &= g_\mathrm{r}(\widetilde{\boldsymbol{F}}^T \otimes \boldsymbol{W}^T)\boldsymbol{R}_2\boldsymbol{G}_\mathrm{t}(\boldsymbol{B}_\mathrm{t}^T \odot \boldsymbol{b}_\mathrm{r}^T)\boldsymbol{Q}, \end{aligned} \tag{16}$$

where $\boldsymbol{F}_2$ is the transmitting pilots matrix satisfying $\boldsymbol{F}_2 = [\boldsymbol{0}, \widetilde{\boldsymbol{F}}]^T$. The matrix $\boldsymbol{R}_2$ can be written as (17).

Obviously, $\boldsymbol{R}_1$ and $\boldsymbol{R}_2$ have the property of rotation invariance below

$$\boldsymbol{R}_2 = \boldsymbol{R}_1\boldsymbol{\Phi}, \tag{18}$$

where $\boldsymbol{\Phi} = \mathrm{diag}\{[e^{j\pi\phi_{\mathrm{t},1}}, e^{j\pi\phi_{\mathrm{t},2}}, \cdots, e^{j\pi\phi_{\mathrm{t},L}}]^T\}$ is the rotation transformation matrix. Such property of rotation invariance is widely employed in the ESPRIT based method [12]. Then we only need to estimate $\boldsymbol{\Phi}$.

By stacking the two received signal matrices, we define

$$\boldsymbol{S} \triangleq \begin{bmatrix} \boldsymbol{X}_1 \\ \boldsymbol{X}_2 \end{bmatrix} = \begin{bmatrix} \boldsymbol{B}_1\boldsymbol{B}_2 \\ \boldsymbol{B}_1\boldsymbol{\Phi}\boldsymbol{B}_2 \end{bmatrix}, \tag{19}$$

where

$$\begin{aligned} \boldsymbol{B}_1 &\triangleq g_\mathrm{r}(\boldsymbol{F}_\mathrm{k}^T \otimes \boldsymbol{W}^T)\boldsymbol{R}_1\boldsymbol{Q}, \\ \boldsymbol{B}_2 &\triangleq \boldsymbol{G}_\mathrm{t}(\boldsymbol{B}_\mathrm{t}^T \odot \boldsymbol{b}_\mathrm{r}^T)\boldsymbol{Q}. \end{aligned} \tag{20}$$

Then, the singular value decomposition (SVD) of the Hermitian matrix $\boldsymbol{S}\boldsymbol{S}^H$ is

$$\boldsymbol{S}\boldsymbol{S}^H = \boldsymbol{U}\boldsymbol{\Sigma}\boldsymbol{U}^H, \tag{21}$$

where $\boldsymbol{U}$ is a unitary matrix and $\boldsymbol{\Sigma}$ is a diagonal matrix whose diagonal entries are the singular values sorted in descending order and the number of the non-zero singular value is L. Thus, we obtain

$$\boldsymbol{U}_{\mathrm{L}} = \begin{bmatrix} \boldsymbol{U}_1 \\ \boldsymbol{U}_2 \end{bmatrix} = \begin{bmatrix} \boldsymbol{B}_1 \\ \boldsymbol{B}_1\boldsymbol{\Phi} \end{bmatrix} \boldsymbol{T}, \tag{22}$$

where $\boldsymbol{T}$ is a linear transformation matrix which is invertible and $\boldsymbol{U}_{\mathrm{L}}$ is the first Lth column vectors of $\boldsymbol{U}$. From (22), we can obtain

$$\boldsymbol{T}^{-1}\boldsymbol{\Phi}\boldsymbol{T} = \boldsymbol{U}_1^{\dagger}\boldsymbol{U}_2. \tag{23}$$

In other words, after we figure out $\boldsymbol{U}_1^{\dagger}\boldsymbol{U}_2$, the diagonal entries of $\boldsymbol{\Phi}$ are the phases of the eigenvalues of $\boldsymbol{U}_1^{\dagger}\boldsymbol{U}_2$, which can be easily obtained through the eigenvalue decomposition (EVD). Then, the AoD of the UE can be estimated.

For the estimation of the AoA of the satellite $\boldsymbol{a}_{\mathrm{r}}$, the mathematical formulation is completely the same as the above so here we do not repeat it again.

According to (11), the AoA and AoD of the RIS has the Khatri-Rao product format $\boldsymbol{B}_{\mathrm{t}}^T \odot \boldsymbol{b}_{\mathrm{r}}^T$ in the received signals. In fact, such Khatri-Rao product format is the same as the usual AoA or AoD matrix, which is

$$\boldsymbol{B}_{\mathrm{t}}^T \odot \boldsymbol{b}_{\mathrm{r}}^T = \begin{bmatrix} 1 & e^{j\pi(\phi_{\mathrm{s}}+\theta_{\mathrm{t},1})} & \dots & e^{j\pi(N_{\mathrm{s}}-1)(\phi_{\mathrm{s}}+\theta_{\mathrm{t},1})} \\ 1 & e^{j\pi(\phi_{\mathrm{s}}+\theta_{\mathrm{t},2})} & \dots & e^{j\pi(N_{\mathrm{s}}-1)(\phi_{\mathrm{s}}+\theta_{\mathrm{t},2})} \\ \vdots & \vdots & \ddots & \vdots \\ 1 & e^{j\pi(\phi_{\mathrm{s}}+\theta_{\mathrm{t},L})} & \dots & e^{j\pi(N_{\mathrm{s}}-1)(\phi_{\mathrm{s}}+\theta_{\mathrm{t},L})} \end{bmatrix}. \tag{24}$$

Consequently, we only need to estimate the matrix $\boldsymbol{B}_{\mathrm{t}}^T \odot \boldsymbol{b}_{\mathrm{r}}^T$ instead of estimating the AoA and AoD of the RIS independently.

Similarly, we first power off the last reflecting element of the RIS and obtain the received signal

$$\begin{aligned} \boldsymbol{Z}_1 &= g_{\mathrm{r}}(\boldsymbol{F}^T \otimes \boldsymbol{W}^T)(\boldsymbol{A}_{\mathrm{t}} \otimes \boldsymbol{a}_{\mathrm{r}})\boldsymbol{G}_{\mathrm{t}}(\boldsymbol{B}_{\mathrm{t}}^T \odot \boldsymbol{b}_{\mathrm{r}}^T)\boldsymbol{Q}_1 \\ &= g_{\mathrm{r}}(\boldsymbol{F}^T \otimes \boldsymbol{W}^T)(\boldsymbol{A}_{\mathrm{t}} \otimes \boldsymbol{a}_{\mathrm{r}})\boldsymbol{G}_{\mathrm{t}}\boldsymbol{P}_1\widetilde{\boldsymbol{Q}}, \end{aligned} \tag{25}$$

where $\widetilde{\boldsymbol{Q}} \in \mathbb{C}^{S\times(N_{\mathrm{s}}-1)}$. $\boldsymbol{Q}_1$ is the RIS phase shifting matrix at the first stage satisfying $\boldsymbol{Q}_1 = [\widetilde{\boldsymbol{Q}}, \boldsymbol{0}]^T$. The matrix $\boldsymbol{P}_1$ has the similar structure of $\boldsymbol{R}_1$ and here we no longer give unnecessary details.

In the second stage, we power off the first reflecting element of the RIS and obtain the received signal

$$\begin{aligned} \boldsymbol{Z}_2 &= g_{\mathrm{r}}(\boldsymbol{F}^T \otimes \boldsymbol{W}^T)(\boldsymbol{A}_{\mathrm{t}} \otimes \boldsymbol{a}_{\mathrm{r}})\boldsymbol{G}_{\mathrm{t}}(\boldsymbol{B}_{\mathrm{t}}^T \odot \boldsymbol{b}_{\mathrm{r}}^T)\boldsymbol{Q}_2 \\ &= g_{\mathrm{r}}(\boldsymbol{F}^T \otimes \boldsymbol{W}^T)(\boldsymbol{A}_{\mathrm{t}} \otimes \boldsymbol{a}_{\mathrm{r}})\boldsymbol{G}_{\mathrm{t}}\boldsymbol{P}_2\widetilde{\boldsymbol{Q}}, \end{aligned} \tag{26}$$

where $\boldsymbol{Q}_2$ is the RIS phase shifting matrix at the second stage satisfying $\boldsymbol{Q}_2 = [\boldsymbol{0}, \widetilde{\boldsymbol{Q}}]^T$. The matrix $\boldsymbol{P}_2$ has the similar structure of $\boldsymbol{R}_2$ and here we no longer give unnecessary details. Similar to $\boldsymbol{R}_1$ and $\boldsymbol{R}_2$, the property of rotation invariance can be written as

$$\boldsymbol{P}_2 = \boldsymbol{P}_1\boldsymbol{\Theta}, \tag{27}$$

Algorithm 1 Two-stage ESPRIT based channel estimation algorithm

1: ***Input***: $\boldsymbol{X}_1$, $\boldsymbol{X}_2$, $\boldsymbol{X}_1$, $\boldsymbol{X}_2$.
2: Stack the received signals as $\boldsymbol{S}$ via (19).
3: Obtain $\boldsymbol{U}$ using SVD via (21).
4: Obtain $\boldsymbol{U}_1$ and $\boldsymbol{U}_2$ via (22).
5: Obtain $\boldsymbol{\Phi}$ using EVD via (23).
6: Reconstruct $\boldsymbol{A}_{\mathrm{t}}$ with $\boldsymbol{\Phi}$.
7: Reconstruct $\boldsymbol{a}_{\mathrm{r}}$ and $\boldsymbol{B}_{\mathrm{t}}^T \odot \boldsymbol{b}_{\mathrm{r}}^T$ with the same steps.
8: Obtain $\widehat{\boldsymbol{H}}$ via (29).
9: ***Ouput***: $\widehat{\boldsymbol{H}}$.

where $\boldsymbol{\Theta} = \mathrm{diag}\{[e^{j\pi(\phi_{\mathrm{s}}+\theta_{\mathrm{t},1})}, \cdots, e^{j\pi(\phi_{\mathrm{s}}+\theta_{\mathrm{t},L})}]^T\}$. Then we only need to replace $\boldsymbol{X}_1$ and $\boldsymbol{X}_2$ with $\boldsymbol{Z}_1$ and $\boldsymbol{Z}_2$ to estimate the rotation transformation matrix $\boldsymbol{\Theta}$ in the same way. Here, we no longer give unnecessary details. After we obtain the complete information of the steering vectors, the channel gain $\boldsymbol{G} \triangleq g_{\mathrm{r}}\boldsymbol{G}_{\mathrm{t}}$ can be estimated as

$$\widehat{\boldsymbol{G}} = \left((\boldsymbol{F}^T \otimes \boldsymbol{W}^T)(\widehat{\boldsymbol{A}}_{\mathrm{t}} \otimes \widehat{\boldsymbol{a}}_{\mathrm{r}})\right)^{\dagger}\boldsymbol{Y}\left((\widehat{\boldsymbol{B}}_{\mathrm{t}}^T \odot \widehat{\boldsymbol{b}}_{\mathrm{r}}^T)\boldsymbol{Q}\right)^{\dagger}. \tag{28}$$

The whole equivalent channel matrix $\boldsymbol{H}$ can be reconstructed as

$$\widehat{\boldsymbol{H}} = (\widehat{\boldsymbol{A}}_{\mathrm{t}} \otimes \widehat{\boldsymbol{a}}_{\mathrm{r}})\widehat{\boldsymbol{G}}(\widehat{\boldsymbol{B}}_{\mathrm{t}}^T \odot \widehat{\boldsymbol{b}}_{\mathrm{r}}^T). \tag{29}$$

This two-stage ESPRIT based algorithm is depicted in Algorithm 1.

B. One-stage null space projection channel estimation

In this subsection, we propose the NSP channel estimation algorithm based on the projection of the dictionary steering vectors to the null space of the received signal covariance matrices. Compared with the ESPRIT based channel estimation algorithm, this algorithm has less resolution but only needs one stage so that it does not need to power on and off any antenna or element. We consider using the signal model (9) to estimate $\boldsymbol{A}_{\mathrm{t}}$ and $\boldsymbol{a}_{\mathrm{r}}$ and the signal model (11) to estimate $\boldsymbol{B}_{\mathrm{t}}^T \odot \boldsymbol{b}_{\mathrm{r}}^T$.

For the estimation of the AoD of the UE, consider a testing vector as

$$\boldsymbol{t}(\phi) = \boldsymbol{F}^H\boldsymbol{\alpha}^*(N_{\mathrm{t}}, \phi), \tag{30}$$

where ϕ can be any value in $[-1, 1]$.

Use the testing vectors to form the uniform dictionary matrix

$$\boldsymbol{D} = \left[\boldsymbol{t}(\phi_1), \boldsymbol{t}(\phi_2), \cdots, \boldsymbol{t}(\phi_N)\right], \tag{31}$$

where $\phi_n = \cos\frac{N-n}{N}\pi, n = 1, 2, \cdots, N$. The angular resolution is $\frac{\pi}{N}$. Note that if we increase the number of the testing vectors N, the angular resolution will increase but the complexity of the matrix calculation will also increase.

From the received signal $\boldsymbol{Y}_s$, we can obtain

$$\boldsymbol{Y}_s^H\boldsymbol{Y}_s = \boldsymbol{F}^H(\boldsymbol{A}_{\mathrm{t}}^T)^H\boldsymbol{C}^H\boldsymbol{C}\boldsymbol{A}_{\mathrm{t}}^T\boldsymbol{F}, \tag{32}$$

where $\boldsymbol{C} = \boldsymbol{W}^T\boldsymbol{H}_{\mathrm{r}}\mathrm{diag}\{\boldsymbol{q}_s\}\boldsymbol{B}_{\mathrm{t}}\boldsymbol{G}_{\mathrm{t}}$. The null space of the matrix $\boldsymbol{Y}_s^H\boldsymbol{Y}_s$ can be written as

$$\mathcal{Z} : \{\boldsymbol{x}|\boldsymbol{F}^H(\boldsymbol{A}_{\mathrm{t}}^T)^H\boldsymbol{C}^H\boldsymbol{C}\boldsymbol{A}_{\mathrm{t}}^T\boldsymbol{F}\boldsymbol{x} = \boldsymbol{0}\}. \tag{33}$$

If $\phi \in \{\phi_{\mathrm{t},1}, \phi_{\mathrm{t},2}, \cdots, \phi_{\mathrm{t},L}\}$, the testing vector $\boldsymbol{t}(\phi)$ will be orthogonal to the null space $\mathcal{Z}$; Otherwise, the projection of the testing vector $\boldsymbol{t}$ in the null space $\mathcal{Z}$ will not be zero. This property inspires us to use different values of ϕ to generate the testing vector $\boldsymbol{t}$ and calculate the projection of $\boldsymbol{t}$ in $\mathcal{Z}$. If the projection is zero, then the value of ϕ is the cosine value of one of the AoD at the UE.

The orthogonal basis of $\mathcal{Z}$ can be obtained through SVD of $\boldsymbol{Y}_s^H \boldsymbol{Y}_s$ written as

$$\boldsymbol{Y}_s^H \boldsymbol{Y}_s = \boldsymbol{V}\boldsymbol{\Gamma}\boldsymbol{V}^H. \tag{34}$$

The singular vectors corresponding to zero singular value in $\boldsymbol{V}$ comprise the orthogonormal basis of the null space $\mathcal{Z}$ denoted as $\boldsymbol{V}_{\mathrm{z}}$. If we assume that $\boldsymbol{Y}_s^H \boldsymbol{Y}_s$ has v zero singular values, then $\boldsymbol{V}_{\mathrm{z}}$ is the last v columns of $\boldsymbol{V}$. Then we can calculate the projection of the testing vector in the null space, which can be written as

$$\boldsymbol{P} = \boldsymbol{V}_{\mathrm{z}}^H \boldsymbol{D}, \tag{35}$$

where $\boldsymbol{P} \in \mathbb{C}^{v \times N}$ is the result of projection. Denote $p_{x,y}$ as the entry in the xth row and yth column of $\boldsymbol{P}$. $\|p_{x,y}\|$ is the projection of the yth testing vector in the xth base vector of the null space $\mathcal{Z}$. Thus, the N diagonal entries of $\boldsymbol{P}^H \boldsymbol{P}$ are the projection of N testing vectors in the null space $\mathcal{Z}$. Then we find the local minimum values of the N projection values, whose indexes are $n_1, n_2, \cdots, n_L$. The estimation of $\boldsymbol{A}_{\mathrm{t}}$ is

$$\widehat{\boldsymbol{A}}_{\mathrm{t}} = \left[\boldsymbol{\alpha}(N_{\mathrm{t}}, \phi_{n_1}), \boldsymbol{\alpha}(N_{\mathrm{t}}, \phi_{n_2}), \cdots, \boldsymbol{\alpha}(N_{\mathrm{t}}, \phi_{n_L})\right]. \tag{36}$$

Note that all the RIS phase shifts $\boldsymbol{q}_s$ do not influence the calculation, which means all the PS time slots can be used to do estimation.

For the estimation of $\boldsymbol{B}_{\mathrm{t}}^T \odot \boldsymbol{b}_{\mathrm{r}}^T$, we use the signal model (11). It has the same mathematical formulation as the above. We only need to replace $\boldsymbol{A}_{\mathrm{t}}$, $\boldsymbol{F}$ and $\boldsymbol{C}$ with $\boldsymbol{B}_{\mathrm{t}}^T \odot \boldsymbol{b}_{\mathrm{r}}^T$, $\boldsymbol{Q}$ and $\boldsymbol{F}^T \otimes \boldsymbol{W}^T)(\boldsymbol{A}_{\mathrm{t}} \otimes \boldsymbol{a}_{\mathrm{r}} g_{\mathrm{r}} \boldsymbol{G}_{\mathrm{t}})$. Then the estimation steps are completely the same as the above. Here, we do not repeat them again.

For the estimation of $\boldsymbol{a}_{\mathrm{r}}$, the corresponding signal model should be

$$\boldsymbol{Y}_s \boldsymbol{Y}_s^H = \boldsymbol{W}^T \boldsymbol{a}_{\mathrm{r}} \boldsymbol{C}\boldsymbol{C}^H (\boldsymbol{W}^T \boldsymbol{a}_{\mathrm{r}})^H, \tag{37}$$

where $\boldsymbol{C} = \boldsymbol{b}_{\mathrm{r}}^T \mathrm{diag}\{\boldsymbol{q}_s\} \boldsymbol{H}_{\mathrm{t}} \boldsymbol{F}$. The null space is

$$\left\{\boldsymbol{x} | \boldsymbol{W}^T \boldsymbol{a}_{\mathrm{r}} \boldsymbol{C}\boldsymbol{C}^H (\boldsymbol{W}^T \boldsymbol{a}_{\mathrm{r}})^H \boldsymbol{x} = \boldsymbol{0}\right\}. \tag{38}$$

The testing vectors can be written as

$$\boldsymbol{t}(\phi) = \boldsymbol{W}^T \boldsymbol{\alpha}(N_{\mathrm{r}}, \phi), \tag{39}$$

where ϕ can be any value in $[-1, 1]$. Then the estimation problem is completely the same as the above. Here, we do not repeat it again.

Similarly, the channel gain can be estimated using (28) and the whole equivalent channel can be estimated using (29). This one-stage NSP based channel estimation algorithm is depicted in Algorithm 2.

Algorithm 2 One-stage NSP based channel estimation algorithm

1: ***Input***: $\boldsymbol{Y}_{p,s}$,N
2: Obtain $\boldsymbol{D}$ via (31).
3: Obtain $\boldsymbol{Y}_s^H \boldsymbol{Y}_s$.
4: Obtain SVD of $\boldsymbol{Y}_s^H \boldsymbol{Y}_s$ via (34).
5: Obtain $\boldsymbol{P}$ via (35).
6: Obtain $\widehat{\boldsymbol{A}}_{\mathrm{t}}$ via (36).
7: Obtain $\widehat{\boldsymbol{a}}_{\mathrm{r}}$, $\widehat{\boldsymbol{B}}_{\mathrm{t}}$ and $\widehat{\boldsymbol{b}}_{\mathrm{r}}$ with the same steps.
8: Obtain $\widehat{\boldsymbol{H}}$ via (29).
9: ***Ouput***: $\widehat{\boldsymbol{H}}$.

IV. Numerical Results

In this section, we evaluate the channel estimation performance for the mmWave MIMO GEO satellite communication system with RIS. We set $N_{\mathrm{r}} = 16$, $N_{\mathrm{s}} = 16$, $N_{\mathrm{t}} = 8$ and $N_{\mathrm{RF}} = 4$. We use the QPSK modulation, where the pilot symbols, i.e., the entries of $\boldsymbol{f}_p$, are randomly selected from $\{-1, 1, i, -i\}$. The phase shifts $\beta_1, \beta_2, \cdots, \beta_{N_{\mathrm{s}}}$ are randomly selected from $[0, 2\pi]$. The carrier frequency is 28GHz. The antenna element gain satisfies $G_{\mathrm{r}} = G_{\mathrm{s}} = 5$dBi [13]. The altitude of the GEO satellite is 3.5786×10^7m. Noise term $\kappa T B_{\mathrm{W}}$ in (5) is normalized in the noise power. The entries of the combine matrix $\boldsymbol{W}$ independently obey the unit complex Gaussian distribution. We set the number of the path from the UE to the RIS $L = 3$. The AoA of the satellite is $60°$. The AoDs of the UE are $15°$, $45°$ and $60°$. The AoAs of the RIS are $20°$, $40°$ and $80°$. The AoD of the RIS is $75°$. For the NSP channel estimation algorithm, we set the size of the dictionary $N = 180$, which means the resolution of the angle is $1°$. The normalized mean squared error (NMSE) is defined as

$$\mathrm{NMSE} \triangleq \mathbb{E}\left\{\frac{\|\widehat{\boldsymbol{H}} - \boldsymbol{H}\|_F^2}{\|\boldsymbol{H}\|_F^2}\right\}. \tag{40}$$

Firstly, we fixed $P = 32$ and $S = 32$, satisfying $PS \geq \frac{N_{\mathrm{r}} N_{\mathrm{s}} N_{\mathrm{t}}}{N_{\mathrm{RF}}}$.As shown in Fig. 2, we provide performance comparisons for the cascaded channel estimation. It is seen that in low SNR, the ESPRIT based channel estimation algorithm has higher accuracy compared with LS and NSP channel estimation algorithm. When SNR is 0dB, the ESPRIT method has 34.43% and 32.76% performance improvement compared with LS and NSP. When SNR is 10dB, the performance of NSP algorithm is 35.54% better than the LS method. Note that the LS and NSP method only need one stage while the ESPRIT method needs two stages.

As shown in Fig. 3, we compare the channel estimation performance of the two-stage ESPRIT channel estimation algorithm in terms of the number of the time slots. It is seen that when SNR is 0dB, the performance improves 31.26% if the number of time slots changes from $P = 2, S = 2$ to $P = 6, S = 6$. When the SNR is 10 dB, the NMSE performance is 0.1124 with $P = 12, S = 12$, which has high accuracy. The performance improves little when $P \geq 12, S \geq 12$.

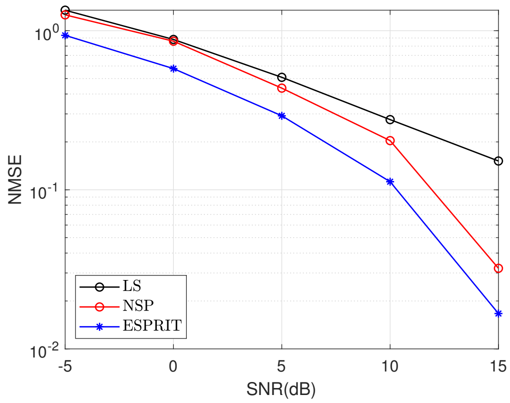

Fig. 2. Comparison of the channel estimation performance in terms of SNR.

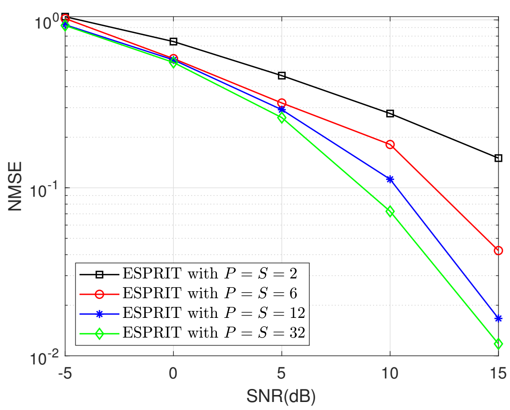

Fig. 3. Comparison of the channel estimation performance for ESPRIT in terms of the number of time slots.

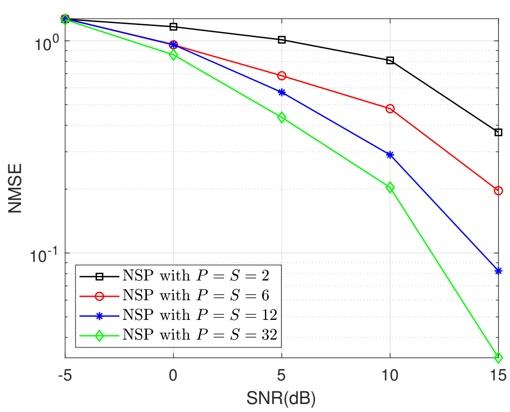

Fig. 4. Comparison of the channel estimation performance for NSP in terms of the number of time slots.

As shown in Fig. 4, we compare the channel estimation performance of the NSP channel estimation algorithm in terms of the number of the time slots. It is seen that the performance improves 26.18% if the number of time slots changes from $P = 2, S = 2$ to $P = 32, S = 32$ when SNR is 0dB. The performance improves 42.41% if the number of time slots changes from $P = 6, S = 6$ to $P = 32, S = 32$ when SNR is 10dB. Thus, compared with ESPRIT, the NSP channel estimation algorithm is more sensitive to the noise and the number of time slots because it involves the calculation of the projection and the signal space.

V. Conclusion

In this paper, we apply the ESPRIT in the mmWave GEO satellite MIMO communication system with RIS to estimate the cascaded channel using two stages. In order to reduce the required stages, we propose the NSP channel estimation algorithm which only needs one stage. Simulation results show that the NSP scheme needs much fewer pilots and much lower hardware complexity than the ESPRIT scheme but with some sacrifice in channel estimation performance.

Acknowledgment

This work is supported in part by the National Natural Science Foundation of China (NSFC) under Grant 62071116.

References

[1] P. Wei, C. Yang, X. Yang, F. Cao, Z. Hu, Z. Li, J. Guo, X. Li, and W. Qin, “Common-view time transfer using geostationary satellite,” *IEEE Trans. Ultrason., Ferroelectr., Freq. Control*, vol. 67, no. 9, pp. 1938–1945, Sep. 2020.

[2] M. Giordani and M. Zorzi, “Satellite communication at millimeter waves: A key enabler of the 6G era,” in *Proc. 2020 Int. Conf. Comput. Netw. Commun. (ICNC)*, Big Island, HI, USA, Mar. 2020, pp. 383–388.

[3] Z. Lin, M. Lin, J. Wang, Y. Huang, and W. Zhu, “Robust secure beamforming for 5G cellular networks coexisting with satellite networks,” *IEEE J. Sel. Areas Commun.*, vol. 36, no. 4, pp. 932–945, Apr. 2018.

[4] B. Zheng and R. Zhang, “Intelligent reflecting surface-enhanced OFDM: Channel estimation and reflection optimization,” *IEEE Wireless Commun. Lett.*, vol. 9, no. 4, pp. 518 – 522, Apr. 2020.

[5] P. Cheng, L. Gui, Y. Rui, Y. Guo, X. Huang, and W. Zhang, “Compressed sensing based channel estimation for two-way relay networks,” *IEEE Wireless Commun. Lett.*, vol. 1, no. 3, pp. 201–204, June 2012.

[6] X. Yang, C. Wen, and S. Jin, “MIMO detection for reconfigurable intelligent surface-assisted millimeter wave systems,” *IEEE J. Sel. Areas Commun.*, vol. 38, no. 8, pp. 1777–1792, Aug. 2020.

[7] J. He, W. Henk, and J. Markku, “Channel estimation for RIS-aided mmWave MIMO systems via atomic norm minimization,” *IEEE Trans. Wireless Commun.*, vol. 20, no. 9, pp. 5786–5797, Sep. 2021.

[8] K. Ardah, S. Gherekhloo, A. L. F. de Almeida, and M. Haardt, “TRICE: A channel estimation framework for RIS-aided millimeter-wave MIMO systems,” *IEEE Signal Process. Lett.*, vol. 28, pp. 513–517, Feb. 2021.

[9] R. W. Heath, N. Gonzalez-Prelcic, S. Rangan, W. Roh, and A. M. Sayeed, “An overview of signal processing techniques for millimeter wave MIMO systems,” *IEEE J. Sel. Topics Signal Process.*, vol. 10, no. 3, pp. 436–453, Apr. 2016.

[10] J. He, H. Leinonen, H. Wymeersch, and M. Juntti, “Channel estimation for RIS-aided mmWave MIMO systems,” in *Proc. 2020 IEEE Global Commun. Conf. (GLOBECOM)*, Taipei, Taiwan, Dec. 2020, pp. 1–6.

[11] C. Qi, H. Chen, Y. Deng, and A. Nallanathan, “Energy efficient multicast precoding for multiuser multibeam satellite communications,” *IEEE Wireless Commun. Lett.*, vol. 9, no. 4, pp. 567–570, Apr. 2020.

[12] W. Ma, C. Qi, and G. Y. Li, “High-resolution channel estimation for frequency-selective mmWave massive MIMO systems,” *IEEE Trans. Wireless Commun.*, vol. 19, no. 5, pp. 3517–3529, May 2020.

[13] H. Wang, P. Zhang, J. Li, and X. You, “Radio propagation and wireless coverage of LSAA-based 5G millimeter-wave mobile communication systems,” *China Commun.*, vol. 16, no. 5, pp. 1–18, May 2019.